Journal of Quantitative Spectroscopy & Radiative Transfer 238 (2019) 106518

Contents lists available at ScienceDirect

Journal of Quantitative Spectroscopy & Radiative Transfer

journal homepage: www.elsevier.com/locate/jqsrt

Properties of polar mesospheric clouds from ACE satellite infrared spectra

Scott C. Jones [a,*], Peter F. Bernath [a,b], Chris D. Boone [a]

[a] Department of Chemistry, University of Waterloo, Waterloo, ON N2L 3G1, Canada
[b] Department of Chemistry and Biochemistry, Old Dominion University, Norfolk, VA 23529, USA

ARTICLE INFO

Article history:
Received 14 February 2019
Revised 29 May 2019
Accepted 29 May 2019
Available online 30 May 2019

Keywords:
Polar Mesospheric Clouds (PMCs)
Atmospheric Chemistry Experiment (ACE)
Satellite remote sensing
Infrared fourier transform spectroscopy (iFTS)

ABSTRACT

An analysis of the Atmospheric Chemistry Experiment (ACE) infrared Fourier transform spectrometer (FTS) spectra for signatures of Polar Mesospheric Clouds (PMCs) has been carried out by looking for the O-H vibrational mode at $\approx 3240\,cm^{-1}$. PMCs are thought to be indicators of climate change in the mesosphere and have been found to be increasing in recent years. Additionally, there are a number of open questions about the microphysics of the clouds, and their physical properties such as temperature, density, and particle shape and size. ACE has access to the entire infrared spectrum, potentially providing more accurate retrievals of these parameters. Using the T-matrix scattering code, we have made fits to the 3 micron ACE-FTS spectra. The ACE data set yielded 1762 unique occultations; after accounting for false positives, 955 occultations were left. We assumed oblate spheroids with a fixed effective radius of 40 nm and a nominal cloud size of 200 km, and obtained reasonable distributions for temperature, axial ratio and particle density. We expect that the methods presented here will allow a new routine ACE PMC data product to be developed.

1. Introduction

Polar Mesospheric Clouds (PMCs), found at altitudes between about 80 km and 90 km near the mesopause, are composed of ice nano-particles [1,2]. They are most prevalent around the summer solstice in the Northern Hemisphere in June and in December in the Southern Hemisphere when temperatures are lowest in the mesosphere. Ground-based observers refer to PMCs as Noctilucent Clouds (NLCs), due to their shining brightly at evening or morning twilight. PMCs have attracted considerable attention in recent years because they are thought to be indicators of climate change driven by increases in greenhouse gases such as CO_2 and CH_4 [3,4]. As the concentration of CO_2 increases, the mesosphere is predicted to cool [5], causing temperatures to drop below the frost point more frequently and increasing PMC abundances. However, mesopause temperatures have changed very little [6], but water vapor has increased because of increasing methane [3], which produces water by oxidation. The nucleation source for PMCs is thought to be meteoric smoke particles from ablation of meteoroids in the Earth's atmosphere [7]. The physical properties of PMCs, such as particle size, shape and number density, can be used to provide information on atmospheric conditions and dynamics. PMCs are non-spherical ice particles with effective radii of 20–80 nm containing a small amount of mineral dust. PMCs occur at temperatures below about 150 K [7–11].

PMCs have been studied through ground, rocket and space observations with increasing sophistication. Most recently, NASA's AIM/SOFIE (Aeronomy of Ice in the Mesosphere/Solar Occultation For Ice Experiment) [12] and AIM/CIPS (Cloud Imaging and Particle Size) [13] instruments have been able to study key PMC characteristics. The Optical Spectrograph and Infrared Imaging System (OSIRIS) on the Odin satellite has been able to assess the vertical and horizontal structure of PMCs using seven different UV wavelengths, confirming that larger, heavier particles sediment to a cloud's lowest layers [14,15]. The Michelson Interferometer for Passive Atmospheric Sounding (MIPAS) instrument on board the Envisat satellite was able to derive ice volume densities, at all times of day, from infrared emission signatures [16]. From the ground, lidar measurements, from both the Southern [17] and Northern [18] Hemispheres, have been used to detect larger PMC particles and their size distributions.

Eremenko et al. [10] carried out an analysis of Atmospheric Chemistry Experiment Fourier Transform Spectrometer (ACE-FTS) and OSIRIS PMC spectra. They examined ≈ 30 spectra from 2004 at polar latitudes and tangent altitudes between 75 and 85 km. One of the primary conclusions was that these clouds predominantly con-

* Corresponding author.
E-mail address: sjones@scisat.ca (S.C. Jones).

https://doi.org/10.1016/j.jqsrt.2019.05.029

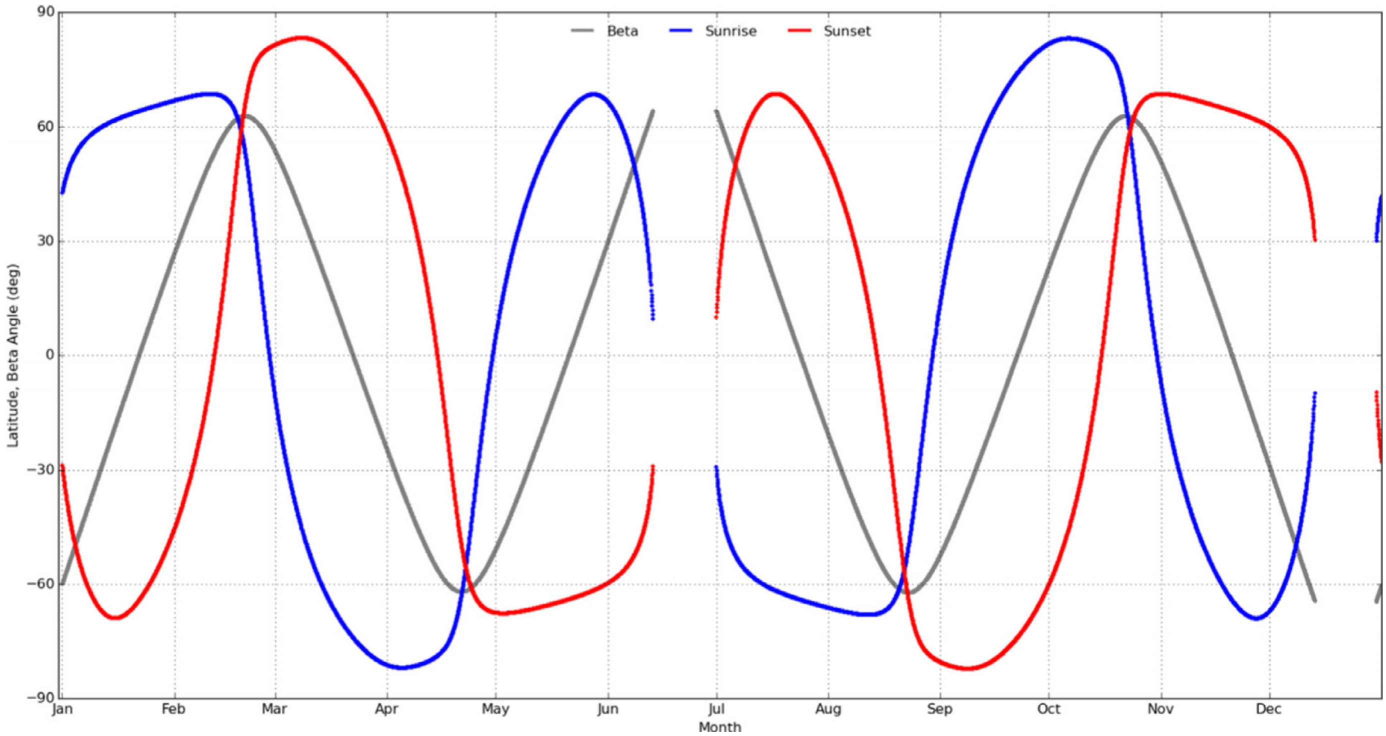

Fig. 1. The latitude and beta angle sampling of ACE occultations for one year (2015).

tained non-spherical ice particles with equivalent average radii of 59 ± 5 nm.

Here, we will present the results of an analysis of all ACE-FTS spectra, from 2004 to the present. The ACE spectra in the 3 micron region were fit with a model to obtain as much information as possible. Section 2 describes the ACE-FTS on board SCISAT and the advantages that it offers in its ability to detect and analyze PMCs. Section 3 explains the methods used to identify PMCs and how the T-matrix algorithm of Mishchenko and Travis [19] was used to fit the spectra. Our results are shown in Section 4, with a comparison to other missions presented in Section 5. Finally, Section 6 offers conclusions and suggestions for future work.

2. ACE-FTS

The Atmospheric Chemistry Experiment (ACE), launched in August 2003, has an infrared Fourier transform spectrometer (FTS) as its primary instrument [20]. ACE-FTS makes high-resolution (0.02 cm^{-1}) spectral measurements in solar occultation mode, covering 750–4400 cm^{-1}. The primary goal of ACE was to achieve a thorough understanding of the chemistry underpinning the evolution of ozone in the stratosphere and upper troposphere, especially in the Arctic. Today, the ACE Science Operations Centre (SOC) at the University of Waterloo (UW) provides more than 35 molecular concentrations, and data for 20 additional isotopologues, an achievement that has led to many varied scientific discoveries. Along with the FTS, ACE also has a two-channel solar imaging camera initially designed to detect obscuring clouds and a UV-visible spectrophotometer called MAESTRO [20]. However, their sensitivity is such that PMC signals are often (but not always) comparable to or less than the noise. ACE traverses a low-Earth (650 km), high-inclination orbit (74°), allowing it to probe latitudes from about 85° S–85° N. The coverage of ACE over the course of single year, 2015, is shown in Fig. 1. This pattern repeats annually in latitude [20]. The ACE-FTS field of view is 1.25 mrad or about 3.5 km on the limb at 85 km altitude. The vertical sampling depends on the beta angle of the orbit (the angle between the orbit plane and the Earth-Sun vector) but is in the range of 2–6 km.

The advantages of the ACE-FTS for PMC observations are complete spectral coverage of the strong 3 micron ice feature at high spectral resolution and sensitivity. The complete spectral coverage provides particle shape information [10] and the high resolution allows retrieval of the PMC temperature [21]. In the infrared, the extinction due to the small PMC particles (less than 100 nm in radius) is almost entirely due to absorption, not scattering, so reliable total ice column densities are obtained but little particle size information. The 3 micron OH ice feature is more than an order of magnitude stronger than the HOH bending mode and the librational mode allowing small particles with low number densities to be detected. These small particles have small scattering cross sections in the UV-visible region and low total ice content.

3. Methods

Although PMCs are more abundant at certain latitudes, altitudes and times of year, the entire ACE data set was searched for possible signatures. We registered a detection using the O-H stretch band vibrational mode at $\approx$3240 cm^{-1}, in a manner similar to Petelina and Zasetsky [21,22]. The chosen threshold relative to the background at 2600 cm^{-1} was 0.99 in transmission, at 0.02 cm^{-1} spectral resolution, and all tangent heights from 70–105 km were deemed valid. The ACE signal-to-noise has been estimated as $\approx$100 [10]. Another occultation instrument, SOFIE, reports much higher sensitivities of $10^5 - 10^6$ [23]. However, ACE has access to the entire spectrum from which to identify a PMC signature.

From February 2004–July 2017, this search yielded 1762 unique occultations, and 4262 total spectra. Unfortunately, due to the geometry of the ACE orbit, there is a gap in observations during peak PMC season in both the northern and southern hemisphere (see Fig. 1) that limits this figure. Thereafter, the wavenumber range was restricted to 2800–3550 cm^{-1} and the spectra were

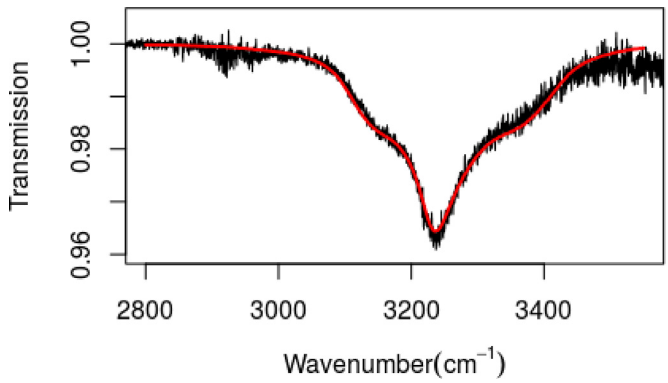

Fig. 2. An example spectrum from the ACE dataset, occultation ss48008, at an approximate tangent height of 84.0 km, fit using the T-matrix code. The temperature, axial ratio, and particle density are 135.8 ± 4.4 K, 2.7 ± 0.1 and 241 ± 14 particles cm^{-3} for a 200 km path length, respectively.

smoothed to 1 cm^{-1} resolution with a Savitzky-Golay filter. The transmission feature was fit in a non-linear least-squares fashion using the T-matrix light-scattering code of Mishchenko and Travis [19]. The code, (available at https://www.giss.nasa.gov/staff/mmishchenko/t_matrix.html) outputs the elements of the normalized scattering matrix along with the extinction cross-section. The T-matrix method is a numerically efficient solution of Maxwell's equations in situations where the wavelength of incoming radiation is on the order of the particle size, and Rayleigh scattering cannot be assumed. It is appropriate for randomly-oriented, rotationally symmetric particle populations, comprised of either single or clustered scatterers. A monodisperse particle distribution with a radius of 40 nm was assumed, the average value found by Hervig et al. [24] in the AIM/SOFIE mission. As can be seen in their Fig. 7, curves of the SOFIE extinction ratios at three different bands converged at 40 nm. Their Fig. 14 shows the highest probability of a radius of 40 nm, low relative to the results of other authors. We tried radii from 40–60 nm, the latter mentioned earlier as the finding of Eremenko et al. [10] from an analysis of OSIRIS spectra. We found the best fits using 40 nm and will use this value going forward. The code models the particles as oblate spheroids (axial ratio greater than 1). With increasing axial ratio, there is a decrease in extinction, leading to shallower and narrower spectral features. At each wavelength an attenuation cross section (μm^2) was calculated using the optical constants of Clapp et al. [25] between 130 and 210 K and supplied to the Beer-Lambert law, assuming a nominal cloud length of 200 km, in order to determine the ice particle number density.

The parameters of interest to the present study are the cloud ice temperature, particle shape (given as an axial ratio (AR)) and the cloud particle density. Temperature and AR are inputs to the T-matrix code; therefore, a set of spectra were pre-calculated for each 0.1 increment of each variable at a spectral resolution of 0.1 cm^{-1}. The atmospheric transmission was calculated using the Beer-Lambert law with a 200 km path length and the cross section for a particular temperature and AR value. A non-linear least-squares routine was used to minimize the observed minus calculated spectra by adjusting the temperature and AR values using the pre-calculated cross section tables and the particle number density. The particle density, n, along the path was allowed to vary between 0–800 cm^{-3}. An example non-linear least squares fit is shown in Fig. 2 for occultation ss48008, at an approximate altitude of 84.0 km. The reported uncertainties have been calculated using the Moore-Penrose inverse, discarding zero singular values. The raw spectrum has been smoothed to a resolution of 1 cm^{-1}.

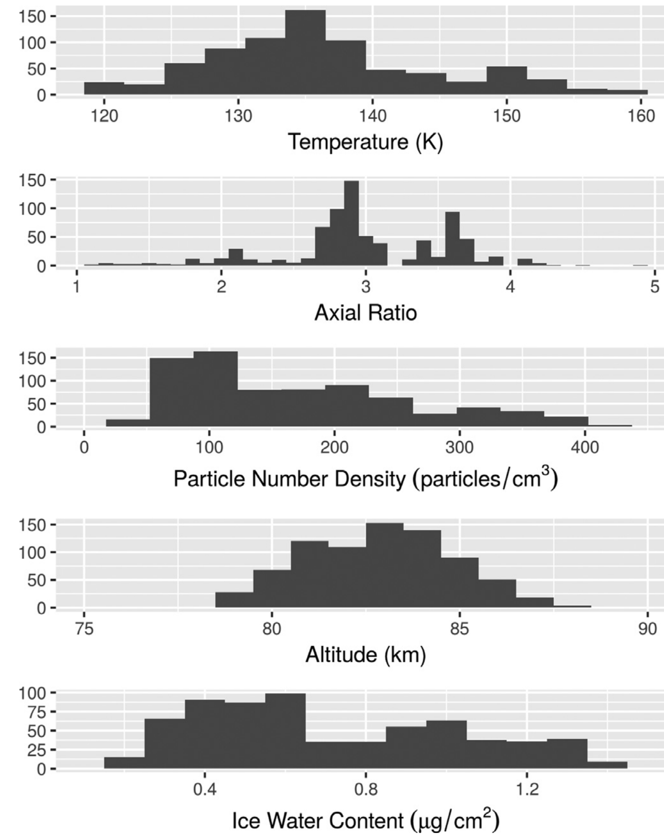

Fig. 3. Distributions of temperature, particle shape (axial ratio), particle density (assuming 200 km path length), altitude and ice water content for ACE spectra recorded from February 2004–July 2017.

4. Results

Occultation ss48008, shown in Fig. 2, recorded a strong PMC detection, at nearly 4% extinction. As a consequence of the relative strength, the detection also appeared in the ACE visible imager, at an altitude of roughly 82 km with a width of 2 km. Other occultations, whose detections may not be significant enough to appear in the imager, may have multiple measurements in which the PMC is registered. In the analysis that follows, only the highest altitude detection will be retained. Due to the geometry of ACE measurements, the highest altitude measurement represents the most accurate estimate of the PMC altitude. At the highest point, the altitude is commensurate with the tangent height of the measurement, while at lower altitudes, where the measurement tangent point is below the cloud, the path length through the cloud field is reduced. (There may be cases where this is not true, for small, isolated clouds that only appear at one altitude in an occultation). However, even the 84.0 km value, for the strongest signal, should be acknowledged as a rough estimate, as the PMC may actually reside in either the foreground or background of the atmosphere through which ACE is measuring. Further, the vertical resolution of ACE-FTS is nearly 4 km and the altitude sampling for this particular occultation is also in this range. Similar to AIM/SOFIE, we have cut off the detections at 79 km at the bottom end, as ice below this level disagrees with most accepted temperature profiles. In addition, any detection at these lower altitudes would likely represent a cloud in the foreground or background of the measurement and not near the tangent point.

Fig. 3 shows the distribution of the parameters of interest across all PMC detections. Fit results had a tendency to bunch up around the extremes for each of the three parameters. Such re-

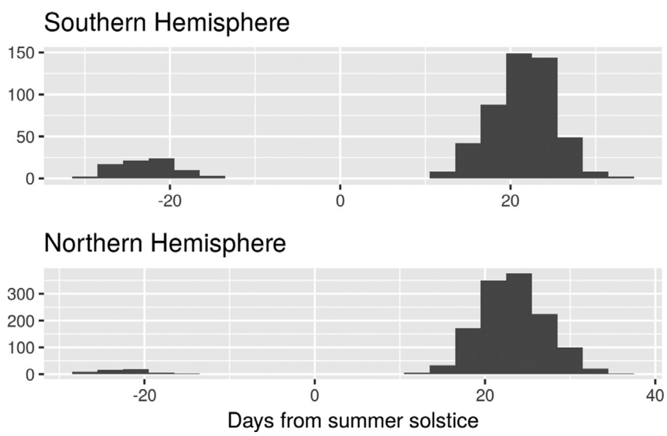

Fig. 4. Measurement dates relative to the respective summer solstices in both hemispheres.

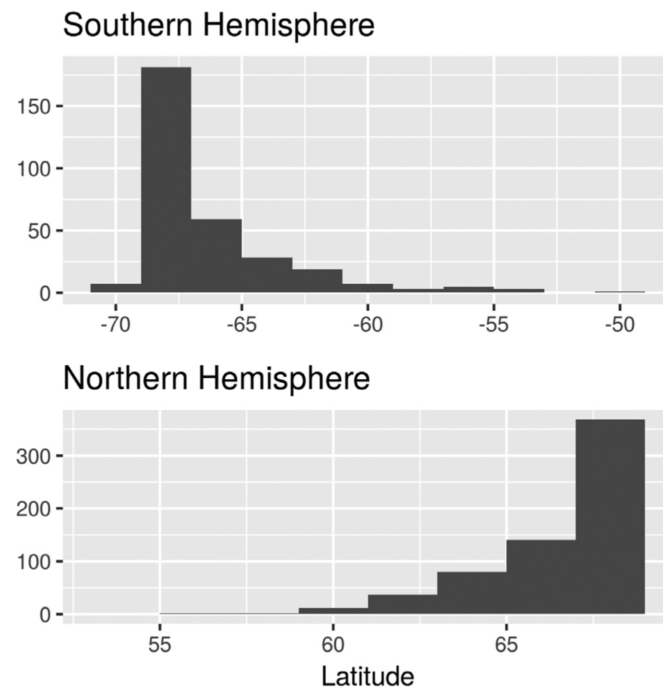

Fig. 5. Latitudes of all PMC detections by hemisphere.

sults were generally indicative of a poor fit and these cases were omitted from further study. The cloud temperature and axial ratio, which appear to peak at $\approx$135 K and $\approx$2.9, respectively, agree reasonably well with the findings of AIM/SOFIE [26] using data from 2008 (see their Figs. 6 and 7). Finally, the volume number density exhibits an exponential drop-off as expected, and peaks at values near those found by MIPAS/Envisat [16] of $\approx$100 particles cm^{-3}. This corresponds to an ACE ice volume density of $\approx 2.7 \times 10^{-2}$ µm^3 ice cm^{-3} ($\approx 2.7 \times 10^{-14}$ cm^3 ice cm^{-3}) given an equivalent radius of 40 nm. A path length of 200 km $= 2 \times 10^7$ cm was assumed so the ice volume column density was typically 5.4×10^{-7} cm^3 ice cm^{-2}. Finally, the ice water content (IWC), integrated over the same path length, comes to $\approx$0.50 µg ice cm^{-2} assuming an ice density of 0.93 g cm^{-3} [27]. The typical SOFIE ice volume density is in the range 10–100 ng m^{-3} or $1\text{–}10 \times 10^{-14}$ g cm^{-3} [24] equivalent to 0.1-1 µg ice cm^{-2} assuming a 200 km path length, similar to that of ACE. Notice that for the ACE slant column retrieval the IWC, axial ratio and ice temperature are reliably determined because they are directly determined from the area, shape and peak position, respectively, of the 3 micron ice feature.

5. Discussion

The Solar Occultation For Ice Experiment (SOFIE) was launched aboard the Aeronomy of Ice in the Mesosphere (AIM) satellite in 2007 in a 600 km sun-synchronous orbit [23]. AIM was designed with the sole goal of measuring PMCs and the surroundings in which they form. Like ACE, SOFIE uses solar occultations to derive extinction, but at 16 wavelength bands from 0.292–5.316 µm. Latitudinal coverage is constrained to 65°–85° (north or south) with 15 Southern Hemisphere sunsets and 15 Northern Hemisphere sunrises each day. PMCs are identified using difference signals from bands close in wavelength. ACE, in contrast, has access to the entire IR spectrum. ACE is less sensitive and has a lower vertical resolution than SOFIE, which has a vertical resolution of 1.5 km and 145 m vertical sampling.

Due to the geometry of the orbit, the latitudes at which ACE makes measurements are polar only $\approx$20–25 days after the solstice in each hemisphere, meaning that only the end of PMC season is captured. The detections recorded are shown in Fig. 4. The corresponding latitudes are shown in Fig. 5. These results, together with the altitude plot of Fig. 3, agree well with previous findings. MIPAS notes PMCs from 81–89 km [16], with increasing frequency towards the poles. Their results also peak at $\sim$84 km. Further, Fig. 1 (bottom) in Karlsson et al. [28] shows that SOFIE anticipates PMCs at lower altitudes, indeed almost at a minimum, during the period that ACE is registering the most detections. Our results of $\sim$83 km at about 20–30 days after solstice match this finding well.

The ACE field-of-view (FOV) is 1.25 mrad; at an observing distance of approximately 2800 km the FOV becomes $\approx$3.5 km. As shown by Hervig et al. [24] and alluded to by Garcia-Comas [16], the bottom and top altitudes of the clouds can be smeared out by the extent of the FOV. In the case of SOFIE, with an FOV of 1.5 km, they predicted a $\sim$1 km adjustment to the cloud boundaries. With an ACE FOV of almost 4 km, it is likely that we are seeing the same effect.

ACE has nearly 15 years of data, however any trend analyses would be quite challenging. Any given PMC season can be highly variable at the time of year and latitude typically sampled by ACE. The sampling allowed by the geometry of the ACE orbit further prevents capturing a maximal number of detections as there are no measurements recorded during much of the peak of the PMC season each year. There will also not be any clear pattern in the number of PMCs detected each year, due to detection problems caused by ice buildup on the detectors in the early years. Moreover, the ACE latitude sampling has drifted by more than 1 week over the course of the mission.

6. Conclusion

The Atmospheric Chemistry Experiment has not produced any information on PMCs since the report of Eremenko et al. in 2005 [10] and the work of Petelina and co-workers [21,22]. Here, we have investigated all ACE data back to mission start using a simple detection scheme based on the presence or absence of the 3200 cm^{-1} O-H stretch band in the spectra. Upon confirmation of this Polar Mesospheric Cloud signature, we used the T-matrix scattering code of Mischenko and Travis [19] in a nonlinear least-squares fit of the spectra, floating the axial ratio (shape) of the particles, their number density, and their temperature. The particle size was fixed at 40 nm, and the shape was chosen to be oblate, rather than prolate. The results were in good agreement with the literature, although given that ACE uses an entire spectrum, the retrievals presented here may be more accurate. The work presented here forms the basis for a new ACE data product.

Acknowledgments

The ACE mission is funded primarily by the Canadian Space Agency.

References

[1] Thomas GE. Mesospheric clouds and the physics of the mesopause region. Rev Geophys 1991;29:553–75.
[2] DeLand MT, Shettle EP, Thomas GE, Olivero JJ. A quarter-century of satellite polar mesospheric cloud observations. J Atmos Sol Terr Phys 2006;68:9–29. doi:10.1016/j.jastp.2005.08.003.
[3] Lubken F-J, Berger U, Baumgarten G. On the anthropogenic impact on long-Term evolution of noctilucent clouds. Geophys Res Lett 2018;45:6681–9. doi:10.1029/2018GL077719.
[4] DeLand MT, Thomas G. Updated PMC trends derived from SBUV data. J Geophys Res Atmosph 2015;120:2140–66. doi:10.1002/2014JD022253.
[5] Roble RG, Dickinson RE. How will changes in carbon dioxide and methane modify the mean structure of the mesosphere and thermosphere? Geophys Res Lett 1989;16(12):1441–4.
[6] Laštovička J, Beig G, Marsh DR. Response of the mesosphere-thermosphere-ionosphere system to global change - CAWSES-II contribution. Prog Earth Planet Sci 2014;1(21). http://www.progearthplanetsci.com/content/1/1/21.
[7] Hervig M, Deaver L, Bardeen C, Russell III J, Bailey S, Gordley L. The content and composition of meteoric smoke in mesospheric ice particles from SOFIE observations. J Atmos Sol Terr Phys 2012;84–85:1–6. doi:10.1016/j.jastp.2012.04.005.
[8] von Cossart G, Fiedler J, von Zahn U. Size distributions of NLC particles as determined from 3-color observations of NLC by ground-based lidar. Geophys Res Lett 1999;26(11):1513–16.
[9] Bailey S, Thomas G, Hervig M, Lumpe J, Randall C, Carstens J, et al. Comparing nadir and limb observations of polar mesospheric clouds: the effect of the assumed particle size distribution. J Atmos Sol Terr Phys 2015;127:51–65. doi:10.1016/j.jastp.2015.02.007.
[10] Eremenko M, Petelina S, Zasetsky A, Karlsson B, Rinsland C, Llewellyn E, et al. Shape and composition of PMC particles derived from satellite remote sensing measurements. Geophys Res Lett 2005;32(L16S06). doi:10.1029/2005GL023013.
[11] Rapp M, Thomas G, Baumgarten G. Spectral properties of mesospheric ice clouds: evidence for nonspherical particles. J Geophys Res 2007;112(D03211). doi:10.1029/2006JD007322.
[12] Gordley LL, Hervig MM, Fish C, Russell III JM, Bailey S, Cook J, et al. The solar occultation for ice experiment. J Atmos Sol Terr Phys 2009;71:300–15. doi:10.1016/j.jastp.2008.07.012.
[13] Lumpe J, Bailey S, Carstens J, Randall C, Rusch D, Thomas G, et al. Retrieval of polar mesospheric cloud properties from CIPS: algorithm description, error analysis and cloud detection sensitivity. J Atmos Sol Terr Phys 2013;104:167–96. doi:10.1016/j.jastp.2013.06.007.
[14] Hultgren K, Gumbel J. Tomographic and spectral views on the lifecycle of polar mesospheric clouds from odin/OSIRIS. J Geophys Res Atmosph 2014;119(14):129–43. doi:10.1002/2014JD022435.
[15] Hultgren K, Gumbel J, Degenstein D, Bourassa A, Lloyd N, Stegman J. First simultaneous retrievals of horizontal and vertical structures of polar mesospheric clouds from odin/OSIRIS tomography. J Atmos Sol Terr Phys 2013;104:213–23. doi:10.1016/j.jastp.2013.06.013.
[16] García-Comas M, López-Puertas, Funke B, Aythami Jurado-Navarro A, Gardini A, Stiller G, et al. Measurements of global distributions of polar mesospheric clouds during 2005–2012 by MIPAS/envisat. Atmos Chem Phys 2016;16:6701–19. doi:10.5194/acp-16-6701-2016. www.atmos-chem-phys.net/16/6701/2016/.
[17] Chu X, Huang W, Fong W, Yu Z, Wang Z, Smith JA, et al. First Lidar observations of polar mesospheric clouds and fe temperatures at mcmurdo (77.8 °s, 166.7 °e), antarctica. Geophys Res Lett 2011;38(L16810). doi:10.1029/2011GL048373.
[18] Baumgarten G, Fiedler J, Rapp M. On microphysical processes of noctilucent clouds (NLC): observations and modeling of mean and width of the particle size distribution. Atmos Chem Phys 2010;10:6661–8. doi:10.5194/acp-10-6661-2010. www.atmos-chem-phys.net/10/6661/2010.
[19] Mishchenko M, Travis L. Capabilities and limitations of a current fortran implementation of the T-Matrix method for randomly oriented, rotationally symmetric scatterers. J Quant Spectros Rad Trans 1998;109:16–21.
[20] Bernath P. The atmospheric chemistry experiment. J Quant Spectros Rad Trans 2017;186:3–16. doi:10.1016/j.jqsrt.2016.04.006.
[21] Petelina S, Zasetsky A. Temperature of mesospheric ice retrieved from the O-H stretch band. Geophys Res Lett 2009;36(L15804). doi:10.1029/2009GL038488.
[22] Petelina S, Zasetsky A. Temperature of mesospheric ice particles simultaneously retrieved from 850 cm^{-1} libration and 3200 cm^{-1} vibration band spectra measured by ACE-FTS. J Geophys Res 2011;116. doi:10.1029/2010JD015050.
[23] Russell III JM, Bailey SM, Gordley LL, Rusch DW, Horányi M, Hervig ME, et al. The Aeronomy of ice in the mesosphere (AIM) mission: overview and early science results. J Atmos Sol Terr Phys 2009;71:289–99. doi:10.1016/j.jastp.2008.08.011.
[24] Hervig M, Gordley L, Stevens M, Russell III J, Bailey S, Baumgarten G. Interpretation of SOFIE PMC measurements: cloud identification and derivation of mass density, particle shape, and particle size. J Atmos Sol Terr Phys 2009;71:316–30. doi:10.1016/j.jastp.2008.07.009.
[25] Clapp M, Miller R, Worsnop D. Frequency-Dependent optical constants of water ice obtained directly from aerosol extinction spectra. J Phys Chem 1995;99:6317–26.
[26] Hervig M, Gordley L. Temperature, shape, and phase of mesospheric ice from solar occultation for ice experiment observations. J Geophys Res 2010;115(D15208). doi:10.1029/2010JD013918.
[27] Pruppacher H, Klett J. Microphysics of clouds and precipitation. Springer Science & Business Media; 2010.
[28] Karlsson B, Randall C, Benze S, Mills M, Harvey V, Bailey S, et al. Intraseasonal variability of polar mesospheric clouds due to inter-hemispheric coupling. Geophys Res Lett 2009;36(L20802). doi:10.1029/2009GL040348.